Resolution Studies of Single-Crystal CVD Diamond

R. Hall-Wilton *CERN,* M. Pernicka *HEPHY Vienna* E. Bartz, J. Doroshenko, D. Hits,S. Schnetzer, R. Stone, *Rutgers University,* V. Halyo, B. Harrop, A. Hunt, D. Marlow, *Princeton University,* W. Bugg, M. Hollingsworth, S. Spanier, *University of Tennessee,* W. Johns, *Vanderbilt University*

***Abstract*—The Pixel Luminosity Telescope (PLT) is a dedicated luminosity monitor, presently under construction, for the Compact Muon Solenoid (CMS) experiment at the Large Hadron Collider (LHC). It measures the particle flux in three layers of pixel diamond detectors that are aligned precisely with respect to each other and the beam direction, utilizing simultaneously performed particle track position measurements. The PLT's single-crystal CVD diamonds are bump-bonded to the PSI46 pixel readout chip - the same readout chip used in the silicon pixel system in CMS. Single-crystal CVD diamond pixel detectors have many attributes that make them desirable for use in charged particle tracking in radiation hostile environments such as the LHC. They are expected to withstand the radiation near the beam pipe over several years at full LHC luminosity with a modest loss of pulse height and no increase of leakage currents. In order to further characterize the applicability of diamond technology to charged particle tracking, the intrinsic spatial resolution of single-crystal CVD diamonds was measured using a high resolution beam telescope developed at the University of Zurich. We present the results of these studies.**

I. Introduction

THE LHC will expose CMS to radiation levels as high as 2×10^{15} protons/cm^2 at the location of the innermost silicon pixel layer (distance to beam $r = 4$ cm). The silicon detectors of CMS are designed to withstand the radiation at the highest luminosity for a time of three years. Under adverse beam conditions with higher radiation levels the lifetime of instruments is reduced, or they can be damaged. It is therefore important to measure the particle flux in order to provide instrument protection via interlocks, issue fast beam aborts, and to provide monitoring data for shifters to establish safe beam conditions over time. In order to operate in such adverse radiation conditions, novel detector technologies must be used. One emerging technology which addresses this problem is CVD diamond detector devices. These devices are radiation hard, have good signal/noise separation, and do not need to be cooled in order to operate.

II. Monocrystalline Diamond Detector

Diamond sensors are crucial application in high radiation environments such as the CMS experiment at the LHC since they will operate efficiently with only moderate decrease in signal size over the entire lifetime of CMS [3]; they are capable of surviving up to 2×10^{15} protons/cm^2. Of equal importance, this radiation hardness does not require that the sensors be cooled. Furthermore, full charge collection is achieved with an electric field between 0.2 V/μm and 0.4 V/μm. Monocrystalline diamond is used for the sensor material rather than polycrystalline diamond since the pulse height distribution of monocrystalline diamond is large and well separated from zero, ensuring that any efficiency changes due to threshold drifts will be small. A comparison of the charge collection properties for both types of diamond is shown in Fig. 1.

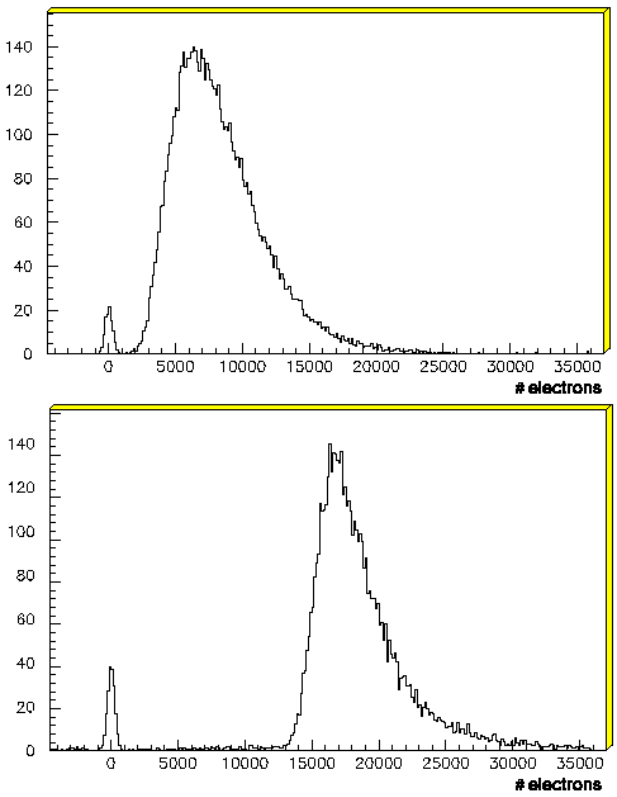

Fig. 1. Charge deposit distributions for electrons from a ^{90}Sr source in polycrystaline CVD diamond (top) and monocrystalline CVD diamond (bottom).

III. Detector Readout

The readout planes consist of monocrystalline diamond sensors. Each sensor is configured with a pixel pattern electrode and bump bonded to the PSI46v2 CMS pixel readout chip [2]. The reason for using pixels is to reduce the capacitance of each channel and, thereby, the inherent serial noise so that the sensor can be read out in the bunch crossing time of 25 ns. Furthermore, it allows to measure tracks for high precision detector alignment and to re-define the active area by masking individual pixels. A schematic drawing of a fully constructed sensor is shown in Fig. 2.

Speaker and contact: hollings@cern.ch

Deposition of the pixel electrode pattern on the diamonds and the bump-bonding of the diamond sensors to the pixel readout chips were performed at the Princeton Institute of Science and Technology Materials (PRISM) micro-fabrication laboratory. Following surface preparation, electrodes were sputtered onto the diamond surface using a Ti/W alloy target as an under bump metalization (UBM). A 4 mm×4 mm electrode was deposited on one side of the diamond using a shadow mask. On the other side, a pixel pattern was deposited using a standard lift-off photolithographic process. The pattern covered an area of 3.9 mm×4.0 mm and consisted of an array of 26 × 40 pixels with pitch of 150 μm × 100 μm matching that of the PSI46v2 chip.

The PSI46v2 chip features individual pixel threshold/mask settings, full analog readout of the pixel hit address and charge deposit, as well as a column-multiplicity signal (known as the fast-or), which indicates the number of double columns that had pixels over threshold in each bunch crossing. These signals may be used as triggers or to make measurements of luminosity; for example, the primary luminosity measurement of the PLT is based on counting the number of telescopes with three-fold coincidences formed from the fast-or output. Fast-or signals are read at bunch-crossing rate of about 40 MHz, while the full pixel information, consisting of the row and column addresses and the pulse heights of all pixels over threshold, is read out at a lower rate of a few kHz. The full pixel readout provides tracking information and is a powerful tool for determining systematic corrections, calibrating pixel efficiencies and measuring the real-time location of the collision point centroid.

The detector readout is done in the same manner as for the CMS silicon pixel detectors, which includes a Front End Driver (FED) and Front End Controller (FEC) [4]. The signals for each telescope plane will be sent over standard CMS optical fiber analog links to the electronics room where a three-fold coincidence for each telescope will be formed.

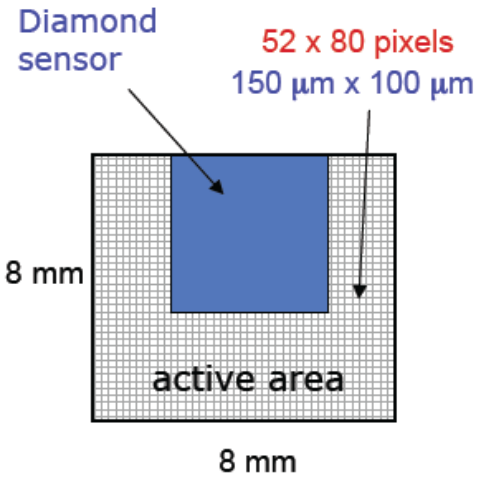

Fig. 2. A schematic drawing of the diamond detector as placed on the CMS pixel readout chip.

IV. Spatial Resolution

The spatial resolution was measured by utilizing a silicon micro-strip telescope provided by the University of Zürich [5] in the 10 GeV/c proton beam at the CERN PS. A single diamond pixel detector was placed in the center of the telescope between two entrance and two exit position modules, each providing an x and y coordinate. This silicon strip telescope has an intrinsic resolution of 2 μm per plane. However, due to multiple scattering effects the position uncertainty at the diamond detector of the reconstructed and selected particle tracks was about 4 μm. Residuals for the PLT were defined as $\Delta_x = x_{track} - x_{plt}$, where x_{track} is calculated from a linear fit to the hits in the silicon strip detectors, and x_{plt} is given as

$$x_{plt} = \frac{\sum_i^N (x_i \cdot Q_i)}{\sum_i^N Q_i} \quad (1)$$

with Q_i the charge in each pixel of the cluster in the PLT, col_i the column address of the pixel, and N the number of hits in the corresponding cluster. The y positions are calculated analogously. The x and y coordinates were treated independently. We apply a correction for non-uniform charge-sharing to the reconstructed hit position as function of the relative charge deposit in the neighboring pixels.

The x and y residuals for 2-hit clusters are shown in Fig. 3. We estimate the resolution from the RMS of theses distributions to be $\sigma_x = 29$ μm (43 μm) and $\sigma_y = 23$ μm (29 μm). The numbers in brackets are the expected corresponding resolutions for single hit clusters.

V. Pixel Luminosity Telescope

The PLT is a dedicated luminosity monitor for CMS based on monocrystalline CVD diamond pixel sensors. It is designed to provide a high-precision measurement of the bunch-by-bunch relative luminosity at the CMS collision point on a time scale of a few seconds and a stable high-precision measurement of the integrated relative luminosity over the entire lifetime of the CMS experiment [7]. The PLT consists of two arrays of eight small-angle telescopes situated one on each end of CMS. Figure 4 shows a three dimensional design drawing of a PLT array. The telescopes consist of three equally-spaced planes of diamond pixel sensors with a total telescope length of 7.5 cm. They are located about 5 cm radially from the beam line at a distance of 1.8 m from the central collision point. Each telescope will be projective at an angle of 1.56° to the interaction point corresponding to a rapidity of $\eta = 4.3$.

VI. PLT Performance Tests

In order to determine the performance of the diamond pixel sensors and the soundness of the PLT design, we carried out tests of a prototype telescope in the 150 GeV/c π^+ beam of the CERN SPS H4 beamline in May of 2009[6], and in 2010 in the 80 GeV/c proton beam in Fermilab's MTEST facility and with the 10 GeV/c proton/pion beam of the CERN PS. The primary goals were to determine: the yield of good pixel channels that result from the bump-bonding

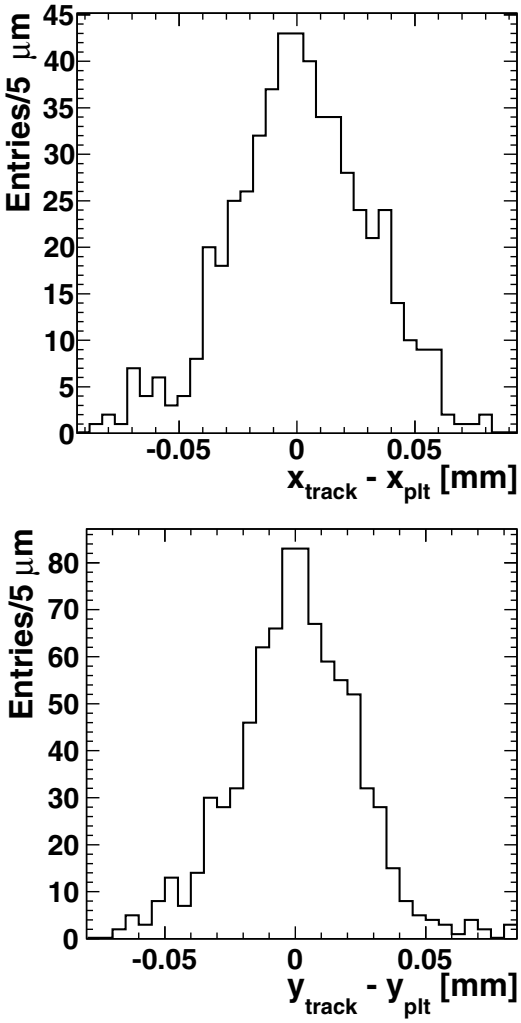

Fig. 3. 2-hit residuals in x and y. For the x residuals, it was required that the hits in the cluster span two columns and no rows, whereas for the y residuals, the opposite was required.

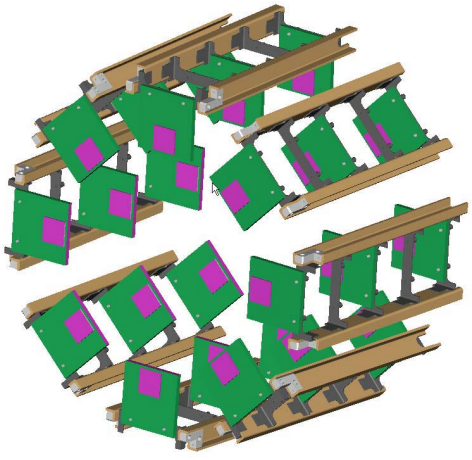

Fig. 4. 3D design drawing of the telescope array at one side of the CMS detector, with the beam pipe in its center not shown. The distance between two outer detector planes is 7.5 cm.

process, the pulse height response of the diamond sensors for minimum ionizing particles, the Fast-OR signal efficiency, and the tracking capability of the diamond pixel planes. Figure 5 shows a three-layer telescope used for the SPS and MTEST test beams. Small scintillators with an active area of 8 mm $\times$ 8 mm were positioned just upstream and downstream of the telescope. All of the results regarding the Fast-OR signals are based on events triggered by a coincidence of these two scintillators.

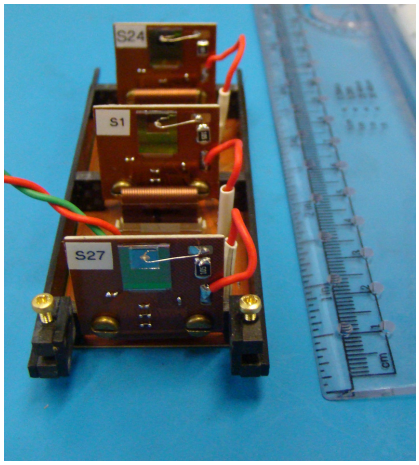

Fig. 5. A fully assembled telescope. The diamond detector sits on top of the ROC and is attached to the high voltage supply wire.

Before taking data, a procedure, similar to that for the CMS pixel detectors, was used to lower the pixel thresholds as much as possible. It utilizes the charge injection feature of the PSI46 pixel chip[2]: internally the readout chip could be programmed to deposit known amounts of charge into selected pixel channels. Iteratively we adjusted three parameters in the readout chip: the estimated average threshold, the trimming range around this setting, and the trimmed threshold for each individual pixel. The pixel thresholds achieved were in the range between 2,500 and 4,500 electrons. The distribution of the turn-on points for each pixel before and after trimming is shown in Fig. 6.

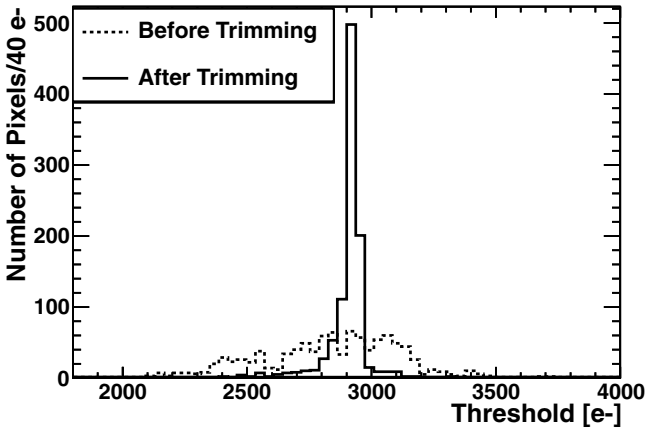

Fig. 6. Distribution of turn-on points in units of collected electrons before and after trimming process.

The telescopes planes were also calibrated using the charge-

injection capability of the PSI46 readout chip. For each pixel, the injected charge was ramped through the full input range while reading the corresponding output signal into the FED. The injected charge was plotted versus the FED ADC value and fit to a second-order polynomial to obtain a mapping from ADC count to pulse height in units of electrons. There is a 10% systematic uncertainty in charge calibration from plane to plane.

For determining charge deposit distributions, we defined an acceptance region which excluded rows or columns with noisy pixels. Figure 7 shows the measured charge distribution in units of collected electrons for single-hit charge clusters. The pulse height plotted is the sum over all neighboring pixels within the hit cluster. The most probable value was found to be 16,500 electrons. For comparison, the most probable signal for a 300 μm thick silicon sensor is 22,000 electrons.

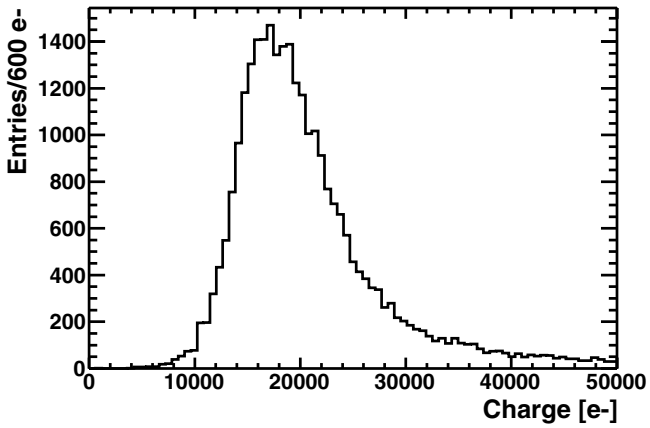

Fig. 7. Summed charge distribution for the plane under test at the CERN PS, 10 GeV/c protons, for single-hit charge clusters. The MPV in units of collected electrons is 16,500.

VII. Fast-OR Signal

The Fast-OR signals form the basis for the primary luminosity measurement of the PLT. Therefore, the measuring the timing response and efficiency is key to establishing their applicability for the PLT. While the Fast-OR output of the PSI46 chip was implemented for possible application in the Level 1 trigger, we present here the first systematic studies of this feature.

Timing and efficiency studies of the Fast-OR signals were performed at a beam test at Fermilab's MTEST using a beam with 80 GeV/c protons and at the CERN SPS with 120 GeV/c $\pi+$.

A. Timing

The timing was studied using a multi-hit TDC which measured the difference between the start of the ADC range in the FED that recorded the Fast-OR in 25 ns bins and the particle arrival, which was defined by the coincidence of two scintillators. The scintillator coincidence was used to trigger the readout of the FED. Both, the FED and the PLT utilize the same global system clock. Hence, this TDC configuration measured the phase between the arrival of a particle and the edge of the global clock. Due to the fixed phase between the trigger and the FED readout, all in-time Fast-OR signals should occur in the same time bin in the FED frame. Figure 8 shows the arrival times of the Fast-OR signals, as measured by the FED. As can be seen most events are in-time events in time-bin 3.

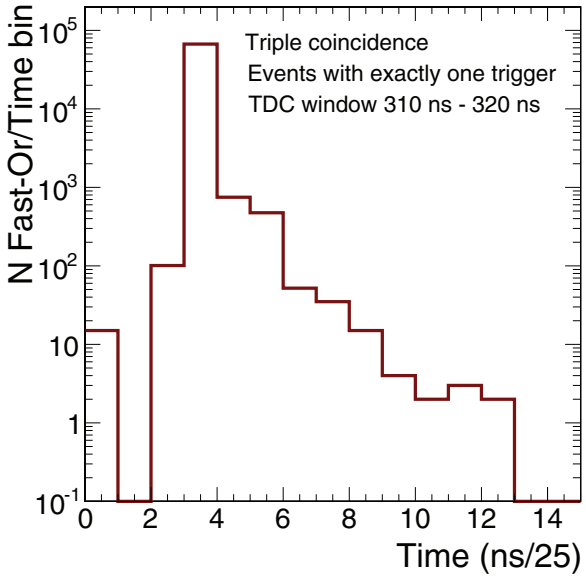

Fig. 8. Arrival time of Fast-OR signal in the FED for all events within a TDC time window of 10ns about 5ns before the next clock cycle. In-time events occur in time-bin 3. Everything to the left of this bin is termed "early" and everything to the right is termed "late".

Due to time-walk, particles which arrive near the clock edge generate a Fast-OR signal either late or early. Late Fast-ORs appear in a 25 ns time bin after the particle arrival in the scintillators, and early Fast-ORs appear in the time bin before the particle arrival. We found two cases: one with single late or early Fast-OR arrivals, called exclusive, and one with an in-time arrival together with a single arrival in a neighboring bin, called inclusive. The percentage occurrence of the late and early Fast-OR signals are summarized in Table I. The exclusive Fast-OR events only affect the bunch-by-bunch luminosity measurement. The inclusive events additionally affect the integrated luminosity measurement. The time walk is related to the pulse-height of the signal which triggered the Fast-OR and the uncertainty of the particle arrival: a particle that arrived shortly after the leading clock edge and that had a large pulse height might be output one clock period earlier than the clock time of the trigger. Similarly, a particle that arrived shortly before the trailing clock edge and that had a small pulse height might be output one clock period later than the clock time of the trigger. The occurrences of such events will be suppressed in the LHC environment due to the particles arriving with a fixed phase with respect to the system clock.

The early and late events were studied further by correlating the TDC information with the arrival time of the Fast-OR signal. The Fast-OR signals tagged as early indeed arrive

	Exclusive	Inclusive
Early	0.13%	0.01%
Late	0.84%	0.38%

TABLE I
SUMMARY OF THE PERCENTAGE OF OCCURRENCE OF EARLY AND LATE FAST-OR SIGNALS. THE VALUES FOR THE LATE ARRIVALS ARE UPPER LIMITS DUE TO CONTRIBUTIONS FROM LATE BEAM PARTICLES.

near the edge of the clock. Late Fast-ORs arrive uniformly distributed in time. This is due to the equal probability of a low pulse height event occurring at any point in time in the 25 ns time bin.

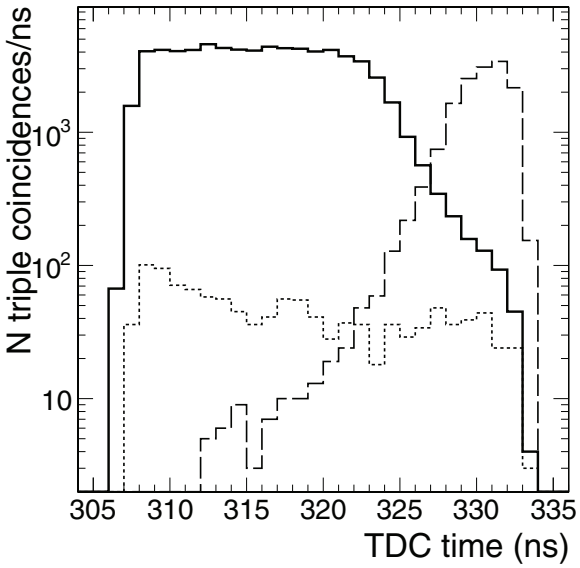

Fig. 9. Fast-OR arrival time with respect to the clock edge, as measured by the TDC. The Fast-OR signals have been divided into in-time (solid line), early inclusive and exclusive (long dashed line), and late inclusive and exclusive (short dashed line) signals.

B. Efficiency

For determining the Fast-OR efficiencies we ensured that a particle passed through the enabled area of the plane under test: single clusters were required in each of the three planes and, for the two planes other than the one under study, the cluster positions were required to be in the central region excluding pixels rows and columns along the boundaries. Rows or columns with noisy pixels were found along the boundary and were excluded as well; this concerned at the most three rows or columns.

In order to correctly determine the Fast-OR efficiency using the test beam data, it is necessary to count Fast-OR signals that occur one clock period early or one clock period late as well as those that occur in-time. The correction due to accidental firing of the Fast-OR signal was found to be negligible. In the nine clock pulses occurring between 2.50 μs and 2.75 μs after a triggered event, there were 87 Fast-ORs out of 100,000 events giving a 0.03% probability for an accidental Fast-OR in a three clock period. The measured efficiencies for each plane were 99.3% for Plane 1, 99.6% for Plane 2, and 99.9% for Plane 3.

VIII. CONCLUSIONS

The CMS detector at LHC extensively uses CVD diamond detectors to monitor and act on adverse beam conditions. As a new addition, the PLT will also provide bunch-by-bunch luminosity measurements at a required relative systematic uncertainty of about 1%. To achieve this it utilizes pixelated monocrystalline CVD diamond detectors. We have completed a preliminary analysis of data from a test of a prototype PLT telescope in a high-energy pion beam. The fraction of active pixel channels in all three planes is 98% or more. The most probable value in the measured pulse height distribution for 150 GeV pions from the SPS at CERN is about 18,000 electrons for a 500 μm thick detector. This is well above the average pixel threshold setting of 2,500 to 4,500 electrons. The efficiency of the fast-or signals that form the basis of the luminosity measurement is greater than 99% for all three planes. Clear and well defined tracks are readily reconstructed in the telescope and allow high precision detector alignments.

The full version of the PLT (2 modules$\times$8 telescopes$\times$3 layers of diamond pixel detectors) is now projected for installation during the Fall 2010 shutdown of LHC.

ACKNOWLEDGMENT

We thank the following people for their contributions to the PLT project: P. Butler, S.P.Lansley, and N. Rodrigues from Canterbury University; L. Lueking from Fermilab; S. Schmid from HEPHY Vienna; Y. Gershtein, E. Halkiadakis, and A. Lath from Rutgers University; B. Sands and D. Stickland from Princeton University; R. Lander from University of California, Davis; and B. Gabela from Vanderbilt University. We thank the staff of the Princeton Institute for the Science and Technology of Materials (PRISM) for their assistance with the bump bonding. We are grateful to the University of Zurich for lending us the strip detector telescope modules. Particularly, the support by C. Regenfus for the electronics readout and J. Rochet for machining a support for the telescope made this test beam possible. We are grateful to CMS Technical Coordination for assistance in launching and sustaining the project, particularly in its early phases. We thank the CERN PS accelerator test beam group and the Fermilab MTEST accelerator test beam group for their excellent operation.

REFERENCES

[1] Bell, Alan. J., "'Beam & Radiation Monitoring for CMS,"' Nuclear Science Symposium Conference Record, 2008. NSS '08. IEEE , vol., no., pp.2322-2325, 19-25 Oct. 2008; W. Lohmann *et al.*, Fast Beam Conditions Monitor BCM1F for the CMS Experiment, Nucl. Instrum. Meth. A 614, 433 (2010).

[2] M. Barbero *et al.*, "'Design and test of the CMS pixel readout chip,"'Nucl. Instrum. Meth. A 517, 349 (2004).

[3] W. de Boer *et al.*, Radiation Hardness of Diamond and Silicon sensors compared. Phys. Stat. Sol. 204, 3004(2007).

[4] D. Kotlinski *et al.*, "'The control and readout systems of the CMS pixel barrel detector,"' Nucl. Instrum. Meth. A 565, 73 (2006).

[5] C. Amsler *et al.*, "A high resolution silicon beam telescope," Nucl. Instrum. Meth. A 480, 501-507 (2002).

[6] R.Hall-WIlton et al, ”Results from a beam test of a prototype PLT diamond pixel telescope”, Nucl. Instrum. Meth. A (2010) , doi:10.1016/j.nima.2010.04.097
[7] E. Halkiadakis, Nucl. Instrum. Meth. A 565, 284 (2006).